Photoelectrical response of hybrid graphene-PbS quantum dot devices

Huang, Y. Q.; Zhu, R. J.; Kang, N.; Du, J.; Xu, Hongqi

Published in:
Applied Physics Letters

DOI:
10.1063/1.4824113

2013

AIP Applied Physics Letters

Photoelectrical response of hybrid graphene-PbS quantum dot devices

Y. Q. Huang, R. J. Zhu, N. Kang, J. Du, and H. Q. Xu

Citation: Applied Physics Letters **103**, 143119 (2013); doi: 10.1063/1.4824113
View online: http://dx.doi.org/10.1063/1.4824113
View Table of Contents: http://scitation.aip.org/content/aip/journal/apl/103/14?ver=pdfcov
Published by the AIP Publishing

Photoelectrical response of hybrid graphene-PbS quantum dot devices

Y. Q. Huang,[1] R. J. Zhu,[1,2] N. Kang,[1,a)] J. Du,[1] and H. Q. Xu[1,3,a)]
[1]*Key Laboratory for the Physics and Chemistry of Nanodevices and Department of Electronics, Peking University, Beijing 100871, China*
[2]*School of Physics and Optoelectronic Technology and College of Advanced Science and Technology, Dalian University of Technology, Dalian 116024, China*
[3]*Division of Solid State Physics, Lund University, Box 118, S-221 00 Lund, Sweden*

(Received 13 August 2013; accepted 16 September 2013; published online 3 October 2013)

Hybrid graphene-PbS quantum dot devices are fabricated on an n-type silicon substrate capped with a thin SiO_2 layer and are characterized by photoelectrical measurements. It is shown that the resistance of the graphene channel in the devices exhibits detectable changes when a laser beam is switched on and off on the quantum dots. The model that explains the observed photoresponse phenomenon is illustrated. We also show that the photoresponse signal, i.e., the photoinduced change in the resistance of the graphene channel can be tuned in both magnitude and sign with a voltage applied to the back gate of the devices and is related to the derivative of the transfer characteristics of the graphene channel. Our work shows that the simple hybrid graphene-PbS quantum dot devices can be employed for photodetection applications. © *2013 AIP Publishing LLC*. [http://dx.doi.org/10.1063/1.4824113]

Graphene, a honeycomb lattice of single layer carbon atoms, has attracted great attention in recent years, because of its unique electronic structure[1,2] and two-dimensional nature of electron transport.[3–6] The valence and conduction bands in graphene touch at a Dirac point and show a linear dispersion relation around the Dirac point. Thus, carriers in graphene behave as relativistic massless Dirac fermions. Given the fact that the carriers in graphene have an extremely high mobility and that photogenerated electrons and holes in graphene have a very short recombination time, graphene layers have been employed to realize ultrafast photodetectors with an operation bandwidth of 40 GHz demonstrated.[7–10]

However, a single pristine graphene layer is only able to absorb about 2% of incident light,[11] which limits its applications in optoelectronics. Efforts have been made to improve the sensitivity of photodetection by either engineering the graphene carrier dynamics or coupling the graphene to optical absorption media.[12–16] For example, photoactive materials, such as inorganic semiconductors,[12] have been brought to contact with graphene. These materials interact strongly with light and can act as efficient photon absorbers. Other studies have demonstrated enhanced photoresponse signals under light excitation at a graphene junction, suggesting that hot carrier and photothermoelectric effects may play a role in the photoresponse of graphene based devices.[15,16] Surface plasmons have also been employed to enhance the optoelectronic response and to reshape the spectral responsivity in graphene.[17,18] However, due to the lack of a carrier multiplication process, the efficiency of photoresponse of pristine graphene devices is still limited to small values of up to quantum efficiency. Recently, hybrid graphene-quantum dot devices have received an increasing interest.[19–22] Due to a long lifetime of the trapped charge carriers in quantum dots and ultrahigh carrier mobility in graphene, a gain of up to 10^8 electrons per photon and a photonic responsivity of $\sim 10^7$ AW^{-1} were demonstrated with these hybrid systems.[19] Later on, similar experiments were carried out on CVD-grown graphene, revealing potential for practical applications.[20] However, a systematic study of the tunability of the devices and the physical process that governs the photoresponse in such hybrid devices still need to be carried out.

In this letter, we report on the realization of graphene-PbS quantum dot (QD) hybrid photodetection devices and the measurements of their photoelectrical response. The measurements show that the photoresponse signal can be sensitively controlled by applying a voltage to the gate fabricated on the back side of the substrate and is related to the derivative of the transfer characteristics of the graphene channel in the devices. We explain our experimental results based on a polarity-dependent carrier transfer model in which photoinduced carriers of one charge polarity in QDs are transferred to the graphene, leading to an accumulation of carriers of the opposite charge polarity in the QDs and thus a change in the carrier density in the graphene, i.e., a photoinduced gating effect on the graphene.

In the hybrid devices, graphene sheets were obtained by a mechanical exfoliation method using bulk Kish graphite and transferred onto a heavily doped, n-type Si substrate with a 280-nm-thick SiO_2 cap layer on top and a predefined back-gate electrode at bottom. The single-layer nature of graphene sheets was confirmed by Raman spectroscopy measurements. The transferred graphene sheets were patterned to a ribbon structure, with a channel width of 1.0 μm and a length of 1.0 μm, using electron-beam lithography (EBL) followed by reactive ion etching. The source and drain contact electrodes were then defined to the graphene (to realize the graphene transistor structures) using a second step of EBL, evaporation

a)Authors to whom correspondence should be addressed. Electronic addresses: nkang@pku.edu.cn and hqxu@pku.edu.cn

of Ti/Au, and a lift off process. The colloid PbS QDs, which were coated with oleic acid to avoid aggregation, were originally dispersed in toluene with a concentration of 5 mg/ml. The deposition of the QDs on the as-prepared graphene transistors were achieved by directly castdropping the QD solution and letting it dry in air or a stream of N_2 gas. The deposition process was monitored by the measurements of resistance changes of the graphene transistors. To improve the coupling between the QDs and the graphene sheets, a small amount of ethanol was also applied to the devices. The above QD deposition process was repeated in other two times before following-up measurements. The resulting density of QDs on the devices was estimated to be $\sim 25\ \mu g/cm^2$. Figure 1(a) displays a schematic for the fabricated graphene-QD hybrid structures, where a graphene field effect transistor (FET) and overlying colloid QDs, serving as conducting path and photon absorber, respectively, are shown. Figure 1(b) shows the results of room-temperature photoluminescence (PL) measurements of the PbS QDs before their deposition on the graphene. Here, an IHR550 grating spectrometer with a liquid N_2 cooled InSb diode was used for photon detection and a 442 nm wavelength He-Cd laser was used for excitation. In Fig. 1(b), a characteristic PL peak of the PbS QDs at about 1400 nm can be clearly identified.

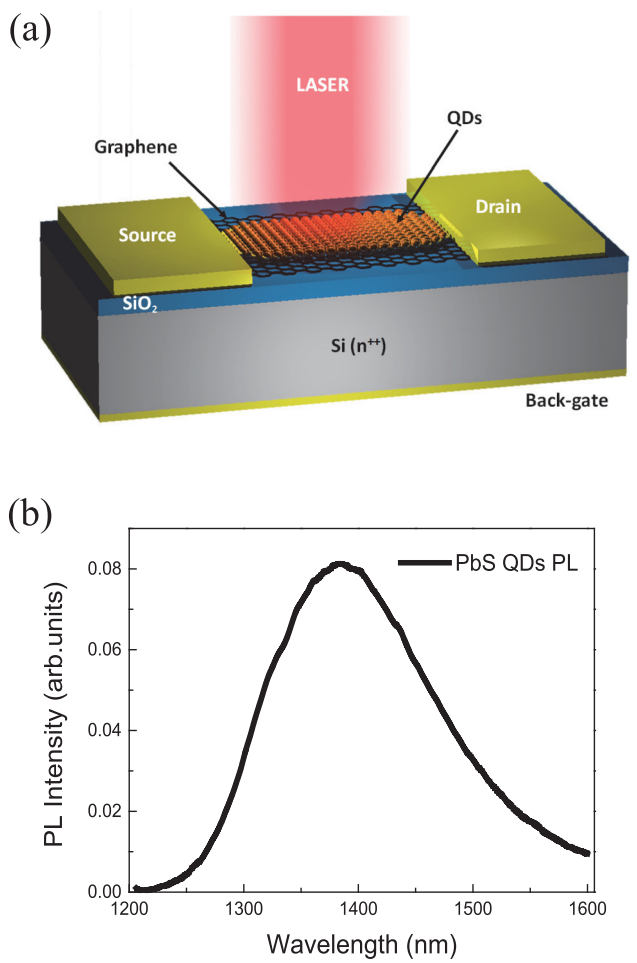

FIG. 1. (a) Schematics of the architecture of the hybrid PbS quantum dots/graphene device. (b) Photoluminescence spectra acquired from the PbS QDs sample used in our experiments with 442 nm laser excitation.

The photoelectric response measurements of the fabricated graphene-PbS QD hybrid devices were preformed using the same laser source for excitation, and a standard DC or lock-in amplification technique for the record of photoelectric response. The laser beam was attenuated and projected onto the devices with a spot size of about 1 mm in diameter. All the measurements were performed at a room temperature, ambient environment.

Figure 2(a) shows the response of the resistance of an as-fabricated hybrid device in the linear transport regime using the lock-in technique by switching the illumination laser light on and off repeatedly. Here a voltage of $V_g = -10\,V$ was applied to the back gate of the device and the graphene was in the hole conduction condition. It is seen that when the device was illuminated, the resistance was rapidly dropped and stayed at a low value level (ON state). The device resistance recovered to its high value level once the illumination laser beam was turned off (OFF state). The observed resistance response was highly reproducible and no significant degradation in the transition of the resistance was seen after many cycles of on and off operations. The overall resistance is seen

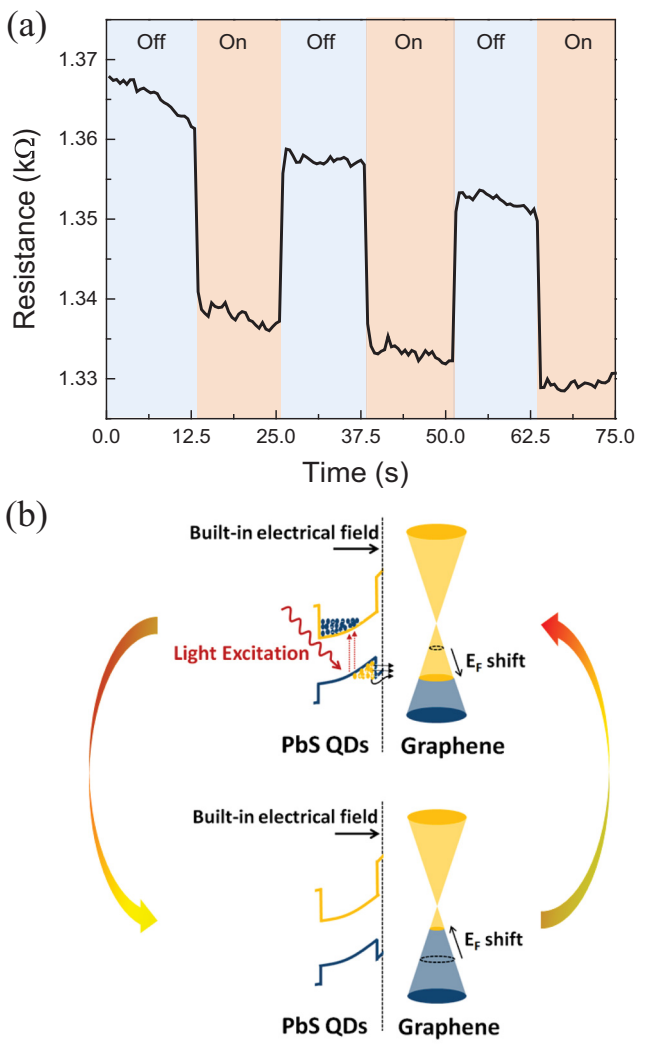

FIG. 2. (a) Temporal resistance response of a typical hybrid PbS quantum dots/graphene device while switching the laser light on and off, taken at gate voltage of $V_g = -10\,V$ and source-drain bias of $V_{sd} = 100\mu V$. (b) Schematic diagram of the photoresponse mechanisms of hybrid device under laser illumination and in the dark.

in Figure 2(a) to decrease with time in the device. This could be attributed to a temporal effect of slow release of deep trapped charge carriers from the quantum dots to the graphene channel. We note that a similar resistance switching behavior has recently been reported for graphene-QD hybrid devices.[19–21] We also note that we have measured graphene FET devices made without deposition of PbS QDs and no photoinduced change in the resistance was observed in a sequence of laser illumination pulses, confirming that the observed photoelectrical response under the laser illumination was indeed due to the presence of the PbS QDs in our fabricated hybrid devices.

Figure 2(b) shows a schematic illustration for the mechanism of the resistance response of the measured graphene-PbS QD hybrid device. The upper panel in the figure shows the physical process when the device is in an ON state. Under laser illumination, the PbS QDs on top of the graphene were excited and electron-hole pairs were created in the QDs. Due to the presence of an electric field, as indicated schematically in the panel, in the hole transport regime, a significant amount of photoinduced hole carriers were transferred to the graphene, leading to a decrease in the Fermi energy in the graphene, an increase in the hole carrier density, and thus an increase in the conductance (or, equivalently, a decrease in the resistance) of the graphene. Furthermore, this hole carrier transfer process resulted in an effective accumulation of electrons in the PbS QDs. As a consequence of this, the Fermi energy in the graphene was further decreased and thus the conductance of the graphene was further increased (a photoinduced electric gating effect). The lower panel in Fig. 2(b) shows the physical situation when the device was in an Off state. When the laser beam was turned off, the process of recombination of electrons and holes took place in the PbS QDs. This led to a decrease in the photoinduced electric gating effect and thus an increase in the Fermi energy. As a result, hole carriers were transferred back to the QDs from the graphene and the conductance of the graphene was decreased. The recovery process continued until the system returned to its original equilibrium condition. As shown in Figure 2(b), we assumed the presence of a built-in electrical field at the graphene-PbS quantum dot interface as a result of charge transfer when the QDs were brought to contact with graphene. The orientation of the built-in electrical field was assumed to be in the direction from PbS quantum dot layer to the graphene, which is consistent with our observed shifts of the charge neutrality point toward negative gate voltage side after the QDs deposition. The strength of the built-in field should depend on the Fermi level in the graphene and thus on a voltage applied to the back gate.

Figure 3 shows the photoelectrical response measurements of the hybrid graphene-PbS QD device at various back gate voltages V_g in the hole transport region of the graphene channel. Here, the measured electrical current passing through the graphene channel under a source-drain voltage bias of $V_{sd} = 0.1\,\text{mV}$ is plotted. It is clearly seen in Fig. 3 that the photocurrent, defined as the ON state current minus OFF state current ($\Delta I_{ph} = I_{ON} - I_{OFF}$), was strongly modulated by the back gate voltage V_g. At $V_g = -2\,\text{V}$, ΔI_{ph} was found to be 0.2 nA. As V_g was decreased, the magnitude of

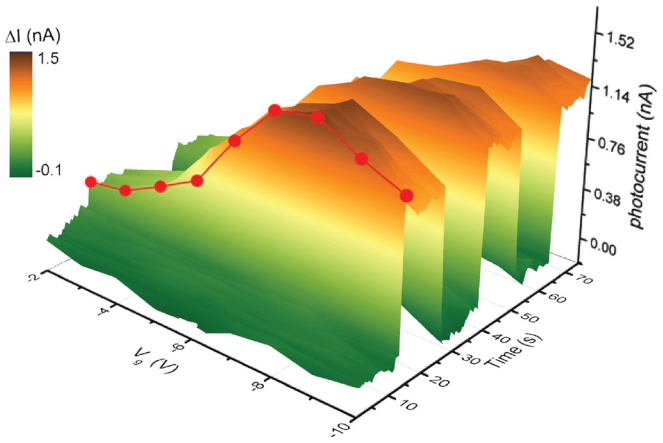

FIG. 3. Time dependence of the photocurrent with switching on/off the laser illumination at various applied gate voltages. The solid curves indicate the gate modulation of photoresponse and the appearance of photocurrent peak around gate voltage of $V_g = -8\,\text{V}$ (The background current in OFF state is subtracted for clearance.).

the photocurrent ΔI_{ph} appeared to be gradually increased. For example, ΔI_{ph} was found to be 0.46 nA at $V_g = -4\,\text{V}$ and reach a value of ~1.36 nA at $V_g = -8\,\text{V}$. After crossing this point, the magnitude of ΔI_{ph} was found to decrease, as V_g was further decreased, and dropped to an indiscernible level at $V_g = -12\,\text{V}$. It is evident that the sensitivity of the photoresponse of our device was back gate voltage-dependent.

Because of the unique ambipolar nature of graphene, charge carriers can be tuned continuously between electrons and holes by changing the gate voltage. When the Fermi level of graphene is turned to the electron transport region, carrier density is reduced with photoinduced lowering of the Fermi energy, in contrast to hole transport region. Therefore, the same photocurrent signal ΔI_{ph}, but with an opposite sign, is expected to be observed in the electron transport region of the graphene channel in such hybrid devices. Figure 4(a) shows the photoresponse measurements of the linear response resistance ($\Delta R_{ph} = R_{ON} - R_{OFF}$) of a device using the lock-in technique under a large range of back gate voltage V_g in which both the hole and the electron transport region of the graphene channel were covered. In the measurements, the laser beam was switched on and off for three times with a light and a dark duration time of 10 s each at every back gate voltage point. Thus, three sets of ΔR_{ph} are presented in the figure and each is plotted as a function of V_g. The results show a good consistency between the three sets of data, indicating that the device exhibited a good repeatability and a capability for a long time operation. As seen in Fig. 4(a), the photoresponse signal showed a negative and a positive maximum at $V_g \approx -10\,\text{V}$ and $V_g \approx 22\,\text{V}$, respectively. In the region between the two maxima, the response signal gradually disappeared as V_g approached to the Dirac point ($V_D = 6\,\text{V}$). The photoresponse signal also slowly approached to zero when V_g moved from the two maxima towards the large bias directions. The same photoresponse behavior was also observed in the measurements of several other fabricated graphene-PbS QD hybrid devices.

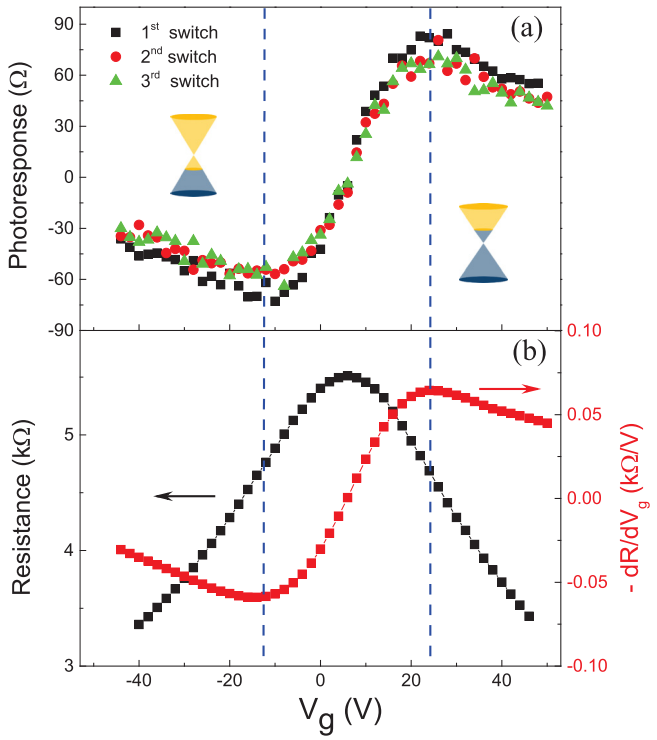

FIG. 4. Comparison of the photoresponse measurement, the resistance, and the transresistance of the same device. (a) Experimentally measured photoresponse as a function of applied gate voltage, V_g. (b) Resistance measurement and the calculated transresistance dR/dV_g (red curve) as a function of V_g. The blue dashed vertical lines are a guide to the eye, highlighting the extremas of the measured photoresponse and dR/dV_g.

Clearly, the overall line shape of the photoresponse signal was antisymmetric with respect to the Dirac point V_D. Based on the physical processes shown schematically in Fig. 2(b), the antisymmetric characteristics of the photoresponse signal were expected to be closely related to the differential of the transfer characteristics of the graphene channel. To verify this, we plot in Fig. 4(b) the measured transfer characteristics of the graphene channel in the device and its first-order derivative $(-dR/dV_g)$ with respect to V_g. As can be seen by comparison the results shown in Figs. 4(a) and 4(b), the photoresponse signal had the same line shape as $-dR/dV_g$ with the positive and negative extrema and the polarity reversing point all coincided with that in $-dR/dV_g$. The photoinduced change in the graphene resistance could be written as

$$\Delta R_{ph} = \frac{\mathrm{d}R}{\mathrm{d}V_g} V_{eff}, \tag{1}$$

where V_{eff} is a light-induced effective voltage which would be applied to the back gate. In our devices, this effective voltage V_{eff} originated from the transfer of photoinduced carriers of one polarity from PbS QDs to the graphene and an accumulation of photoinduced carriers of the other polarity in QDs. It is evident that V_{eff} is a function of the excitation power of the laser beam, the back gate voltage, and the capacitive coupling between the PbS QD layer and the graphene layer. An increase in the magnitude of V_{eff} can be achieved by increasing the excitation power of the laser beam on the device. While at a fixed excitation power, V_{eff} depends on the amount of carriers which could be transferred to the graphene layer from the PbS QDs and thus on the back gate voltage. The latter influences the Fermi energy of the graphene and the potential profile across the QD and graphene layers. Furthermore, an effectively large V_{eff} could also be achieved by placing QDs as close as possible to the graphene layer. A large V_{eff} is desired for a high photoresponse sensitivity of the hybrid device as can be seen in Eq. (1). However, the antisymmetric characteristics of the photoresponse signal ΔR_{ph} are predominantly related to the transfer characteristics of the graphene channel as is seen in Fig. 4. Thus, to achieve an efficient operation with a fabricated graphene-PbS QD hybrid device, it is necessary to tune the back gate voltage to a desirable point in which the magnitude of $\mathrm{d}R/\mathrm{d}V_g$ is large.

In summary, we have fabricated hybrid graphene-PbS QD devices and measured their photoelectric response characteristics. The measurements showed that the photoresponse signal, i.e., the change in the resistance of the graphene channel in each device can be tuned in both magnitude and sign with a voltage applied to the back gate of the devices. The measurements also showed that the characteristics of the photoresponse signal ΔR_{ph} are predominantly related to the transfer characteristics of the graphene channel. A model that explained the physical processes for the observed photoresponse characteristics has been illustrated and discussed. Our work shows that the simple graphene-PbS QD hybrid devices have potential in photodetection applications. The work also demonstrates that the electrical properties of a graphene layer can be effectively modulated using a laser beam and thus provides an additional, optical means of tuning in the study of the transport properties of graphene.

We acknowledge financial support by the National Basic Research Program of the Ministry of Science and Technology of China (Nos. 2011CB933002, 2012CB932703, and 2012CB932700) and by the National Natural Science Foundation of China (No. 91221202). N.K. thanks the Ph.D. Program Foundation of the Ministry of Education of China for financial support (Grant No. 20120001120126). H.Q.X. acknowledges also the financial support from the Swedish Research Council (VR).

[1]K. S. Novoselov, A. K. Geim, S. V. Morozov, D. Jiang, Y. Zhang, S. V. Dubonos, I. V. Grigorieva, and A. A. Firsov, Science **306**, 666 (2004).
[2]A. K. Geim and K. S. Novoselov, Nature Mater. **6**, 183 (2007).
[3]M. I. Katsnelson, K. S. Novoselov, and A. K. Geim, Nat. Phys. **2**, 620 (2006).
[4]K. I. Bolotin, K. J. Sikes, Z. Jiang, M. Klima, G. Fudenberg, J. Hone, P. Kim, and H. L. Stormer, Solid State Commun. **146**, 351 (2008).
[5]K. S. Novoselov, Z. Jiang, Y. Zhang, S. V. Morozov, H. L. Stormer, U. Zeitler, J. C. Maan, G. S. Boebinger, P. Kim, and A. K. Geim, Science **315**, 1379 (2007).
[6]Y. Zhang, Y.-W. Tan, H. L. Stormer, and P. Kim, Nature **438**, 201 (2005).
[7]F. Xia, T. Mueller, Y.-M. Lin, A. Valdes-Garcia, and P. Avouris, Nat. Nanotechnol. **4**, 839 (2009).
[8]T. Mueller, F. Xia, and P. Avouris, Nat. Photonics **4**, 297 (2010).
[9]F. Bonaccorso, Z. Sun, T. Hasan, and A. C. Ferrari, Nat. Photonics **4**, 611 (2010).
[10]P. Avouris, Nano Lett. **10**, 4285 (2010).

[11]K. F. Mak, M. Y. Sfeir, Y. Wu, C. H. Lui, J. A. Misewich, and T. F. Heinz, Phys. Rev. Lett. **101**, 196405 (2008).
[12]H. Chang, Z. Sun, K. Y.-F. Ho, X. Tao, F. Yan, W.-M. Kwok, and Z. Zheng, Nanoscale **3**, 258 (2011).
[13]M. E. Itkis, F. Wang, P. Ramesh, E. Bekyarova, S. Niyogi, X. Chi, C. Berger, W. A. de Heer, and R. C. Haddon, Appl. Phys. Lett. **98**, 093115 (2011).
[14]X. Gan, K. F. Mak, Y. Gao, Y. You, F. Hatami, J. Hone, T. F. Heinz, and D. Englund, Nano Lett. **12**, 5626 (2012).
[15]N. M. Gabor, J. C. W. Song, Q. Ma, N. L. Nair, T. Taychatanapat, K. Watanabe, T. Taniguchi, L. S. Levitov, and P. Jarillo-Herrero, Science **334**, 648 (2011).
[16]X. Xu, N. M. Gabor, J. S. Alden, A. M. van der Zande, and P. L. McEuen, Nano Lett. **10**, 562 (2010).
[17]T. J. Echtermeyer, L. Britnell, P. K. Jasnos, A. Lombardo, R. V. Gorbachev, A. N. Grigorenko, A. K. Geim, A. C. Ferrari, and K. S. Novoselov, Nat. Commun. **2**, 458 (2011).
[18]Y. Liu, R. Cheng, L. Liao, H. Zhou, J. Bai, G. Liu, L. Liu, Y. Huang, and X. Duan, Nat. Commun. **2**, 579 (2011).
[19]G. Konstantatos, M. Badioli, L. Gaudreau, J. Osmond, M. Bernechea, F. P. Garcia de Arquer, F. Gatti, F. H. L. Koppens, and F. P. G. De Arquer, Nat. Nanotechnol. **7**, 363 (2012).
[20]Z. Sun, Z. Liu, J. Li, G.-A. Tai, S.-P. Lau, and F. Yan, Adv. Mater. **24**, 5878 (2012).
[21]D. Y. Zhang, L. Gan, Y. Cao, Q. Wang, L. M. Qi, and X. F. Guo, Adv. Mater. **24**, 2715 (2012).
[22]D. I. Son, H. Y. Yang, T. W. Kim, and W. Park, Appl. Phys. Lett. **102**, 21105 (2013).